Journal of Materials Chemistry B

Accepted Manuscript

ROYAL SOCIETY OF CHEMISTRY

www.rsc.org/materialsB

Folate-targeting redox hyperbranched poly(amido amine)s delivering MMP-9 siRNA for cancer therapy

Mengyi Li [1,a], Xiaoyan Zhou [1,a], Xiaolong Zeng [1], Changyong Wang [1,2], Jiake Xu [3], Dong Ma *[,1], Wei Xue *[,1,4]

[1] Key Laboratory of Biomaterials of Guangdong Higher Education Institutes, Department of Biomedical Engineering, Jinan University, Guangzhou 510632, China

[2] Department of Advanced Interdisciplinary Studies, Institute of Basic Medical Sciences and Tissue Engineering Research Center, Academy of Military Medical Sciences, Beijing 100850, China

[3] School of Pathology and Laboratory Medicine, University of Western Australia, Perth, Australia

[4] Institute of Life and Health Engineering, Key Laboratory of Functional Protein Research of Guangdong Higher Education Institutes, Jinan University, Guangzhou 510632, China

* Co-corresponding authors:

E-mail: madong_jnu@163.com (Dr. D. Ma); Tel/Fax: + 86 20 85224338

weixue_jnu@aliyun.com.cn (Prof. W. Xue); Tel/Fax: + 86 20 85228829

[a] The authors contributed equally to this work.

Abstract

For effective gene delivery to breast cancer MCF-7 cells, a folate-targeting redox gene carrier was synthesized by Michael addition polymerization between 1-(2-aminoethyl) piperazine and *N,N'*-cystaminebisacrylamide. Folate was then conjugated through an amidation reaction. The obtained folate-modified hyperbranched poly(amido amine)s (FA-PAAs) degraded in the presence of glutathione and displayed excellent transfection efficiency *in vitro*. Particularly, FA-PAAs showed much higher gene delivery efficiency than that of PEI-25k in the presence of serum, leading to an obvious decrease in MMP-9 protein expression and the apoptosis of MCF-7 cells. Moreover, FA-PAAs displayed lower cytotoxicity and better blood compatibility than PEI-25k, suggesting a potential application in gene therapy to tumors.

1. Introduction

Cancer has become one of the biggest threats to human health [1-3]. Taking breast cancer as the example, more than 500 thousands women die from breast cancer every year in the world [4]. The commonly used treatment strategies to cancer therapy are chemotherapy, radiotherapy and surgical treatment in clinical. However, surgical treatment is powerless when facing to the transferring lesions, and the chemotherapy and radiotherapy usually bring with severe side effects [5-7].

Gene therapy which is a promising strategy for cancer therapy has attracted much attention in biomedicine recently because this technique can target to cancer cells with safety and efficiency, and almost displays no side effects [8]. For gene therapy, a safe and highly efficient gene carrier is the key factor. A series of cationic carriers such as liposome, PEI, PAMAM have been prepared for gene delivery and cancer therapy [9-11]. Nowadays, challenges remains in preparation of safe and efficient gene carriers for clinical application. For example, liposome shows serious cytotoxicity, and PEI/PAMAM show relative low transfection efficiency [12].

In view of the characteristics of high GSH expression in tumor tissues and cells, some GSH-responsive cationic polymers containing disulfide linkages have been synthesized and used for gene therapy to tumors [13]. These redox cationic polymers can condense DNA and form compact complexes. After enter the cellular cytoplasm, the high GSH concentration results in the breakage of disulfide bonds and the rapid unpacking of DNA from the complexes. Therefore, not only the transfection efficiency is increased due to the release of DNA from the complexes, but also cytotoxicity is reduced because intracellular accumulation of the high-molecular-weight cationic polymers is avoided [14,15].

Among them, the redox hyperbranched poly(amido amine)s (PAAs) consisting of 1-(2-aminoethyl) piperazine and *N,N′*-bis(acryloyl) cystamine is the typical representative and shows the potential application in gene therapy [16]. PAAs can degrade in cancer cells and release DNA in the cytoplasm. More important, the hyperbranched structure of PAAs can improve the transfection efficiency because this hyperbranched structure helps the complexes to escape from the intracellular lysosome [17,18].

To deliver gene to tumor cells more effectively, targeting gene carriers have been developed [19-21]. It is reported that folate receptors (FRs) are expressed at high levels in numerous cancer

cells including breast cancer MCF-7 cells, while expressed at low levels in normal tissues [22,23]. Due to the strong affinity between FRs and folate (FA), many works have been dedicated for folate-targeting gene delivery and good effects were reported [24-26].

In this paper, we designed and synthesized a FA-targeting gene carrier FA-PAAs. *In vitro* assays have been carried out to confirm the target ability of FA-PAAs, and western blot and apoptosis assays display the effective inhibition to MCF-7 cells. In addition, the biocompatibility including blood compatibility of FA-PAAs is also assayed to confirm the safety of the obtained gene carrier.

2. Materials and methods

2.1. Materials

Acryloyl chloride, cystamine dihydrochlorid, 1-(2-aminoethyl) piperazine (AEPZ, 99%), folic acid (FA), *N*-hydroxy-succinimide (NHS, 98%) and dicyclohexylcarbodiimide (DCC) were purchased from Aladdin Industrial Corporation (Shanghai, China). Branched PEI with the average molecular weight of 25 kDa was purchased from Sigma. Cell counting kit-8 (CCK-8) was purchased from Beyotime Institute of Biotechnology (Shanghai, China). All used solvents were purchased from Guangzhou Chemical Reagent (China) and used without further purification. MCF-7 (human breast adenocarcinoma cell line) was obtained from Southern Medical University in Guangzhou. Dulbecco's modified eagle's medium (DMEM) and fetal bovine serum (FBS) were purchased from Invitrogen Corporation (Washington, USA).

2.2. Synthesis of PAAs

For PAAs synthesis, *N,N'*-cystaminebisacrylamide (CBA) was firstly synthesized according to our previous work [27]. In brief, 2.5 g cystamine dihydrochloride was dissolved in 11 mL distilled water. Then, 6.6 mL acryloyl chloride solution in dichloromethane (v/v = 1/1) and 4.4 mL aqueous NaOH solution (0.40 g/mL) were added dropwise with stirring under the ice bath. After that, the mixture was stirred at room temperature for another 6 h. Mixture phase was extracted with dichloromethane and washed by distilled water. Then CBA was obtained with a yield of 82% after the organic solvent was removed under the reduced pressure. ^{1}H NMR ($CDCl_3$): δ = 6.65 (s, 2H, CON*H*CH_2), 6.25 (m, 4H, C*H*$_2$CHCO), 5.62 (m, 2H, CH_2C*H*CO), 3.60 (m, 4H, CONHC*H*$_2$$CH_2$S),

2.92 (m, 4H, $CONHCH_2CH_2S$).

The bioreducible hyperbranced PAAs was synthesized by one-pot two-step Michael addition polymerization of CBA and AEPZ according to reported method [15]. CBA (1.5 mmol) was dissolved in 10 mL methanol/water (v/v = 3/1) solution containing 200 mM calcium chloride at room temperature. AEPZ (0.75 mmol) was then added dropwise to the solution with stirring under a nitrogen atmosphere. The mixture was reacted at 50 ℃ for 30 h. After that, 1.5 mmol AEPZ was added and the mixture was kept reacting at 50 °C for another 8 h. The solvent was removed by rotary evaporation and the residue was dialyzed in distilled water for 3 d (MWCO=3500, USA). The resultant PAAs was obtained by lyophilization with a yield of 54%. ^{1}H NMR (D_2O): δ = 3.60 (m, 4H, $CONHCH_2CH_2S$), 3.30 (m, 4H, NCH_2CHCO), 3.25 (m, 4H, NCH_2CH_2CO), 2.92 (m, 4H, $CONHCH_2CH_2S$), 2.5-2.9 (m, 12H, CH_2 from AEPZ).

2.3. Synthesis of FA-modified PAAs (FA-PAAs)

For the synthesis of FA-modified PAAs, 0.01 g FA was dissolved in 7 mL DMSO, and then 0.02 g DCC and 0.01 g NHS were added. The mixture was reacted for half an hour. After that, 3mL DMSO containing 0.10 g PAAs was added dropwise to the mixture while stirring. The mixture was stirred for 24 h at room temperature in the dark. FA-PAAs was obtained by dialysis and freeze drying with a yield of 70%.

The chemical structure of obtained FA-PAAs was characterized by ^{13}C NMR in D_2O. UV-Visible spectrum was obtained in a 1 cm quartz cuvette using a UV-2550 spectrophotometer (Shimadzu, Japan) at 25 °C. FA, FA-PAAs and PAAs were dissolved in DMSO/water mixture (v/v = 1/99). For GSH-responsibility analysis, 2 mg FA-PAAs was added into the aqueous solution containing 10 or 100 μM GSH. After incubated for 4 or 8 h, the mixtures were analyzed by Gel Permeation Chromatography (GPC) using PEG as the standard. GPC measurements were equipped with a VE 1122 HPLC pump and a Model 270 RI detector using dextran as a standard. The aqueous sodium nitrate (0.8 mol/L) was used as the eluent.

2.4. FA-targeting assay

FA-PAAs was firstly labeled by FITC according to the reported method [28]. The obtained FA-PAAs-FITC was then incubated with MCF-7 cells for FA-targeting exploration. MCF-7 cells

were pretreated without or with 5 μmol/L FA overnight, then seeded onto a 24-well plate (1×10^4 cells/well) with complete DMEM (with high glucose and 10% fetal bovine serum supplemented) in a humidified atmosphere of 5% CO_2 at 37°C. After 24 h, the growth medium was replaced with 200 μL complete DMEM culture medium that contained the desired amount of FA-PAAs-FITC and PAAs-FITC respectively. After 1 h incubation, the formulations were removed and cells were washed with PBS for three times. The ratios of materials uptaken by MCF-7 cells were observed by the fluorescence microscope (Nikon-2000U, Japan), and then digested by trypsinase (0.05% in PBS) for flow cytometry analysis. The uptaken percents (positive cell percent) were calculated by dividing the number of fluorescent cells by the number of total cells in a certain area of a well.

2.5. Complexation with DNA

For the complexation of FA-PAAs with EGFP plasmid (pEGFP), FA-PAAs and MMP-9 were firstly dissolved in ultrapure water to make aqueous solutions with appropriate concentrations. Then, the resultant component solutions were mixed at room temperature, and stirred gently for 20 min for the formation of FA-PAAs/pEGFP complexes.

2.6. *In vitro* transfection

MCF-7 cells were seeded at a density of 1×10^4 cells per well onto 24-well tissue culture plates in complete DMEM (Dulbecco's Modified Eagle Medium) culture medium, and then incubated without or with 5 μmol/L FA overnight in a humidified 5% CO_2 atmosphere at 37°C. After that, the culture medium was replaced by freshly prepared FA-PAAs/MMP-9 (with a weight ratio of 50, 60, 70 and 80 respectively) complexes in serum-free DMEM were added. The MMP-9 plasmid in each well was fixed at 2.0 μg. After 6 h incubation, the formulations were removed and 500 mL of fresh DMEM culture medium was added. The experiments of studying gene transfection were continued to 42 h, and then the cells were analyzed for green fluorescence protein (GFP) expression with a fluorescence microscope (Nikon-2000U, Japan). The cells treated with PEI/MMP-9 (N/P = 10) were set as the control groups. After the cells were digested by trypsinase (0.05% in PBS), the transfection percents (positive cell percent) were calculated by dividing the number of fluorescent cells by the number of total cells in a certain area of a well. The transfection efficiency was recorded by a flow cytometer (Accuri C6).

2.7. MMP-9 protein expression

MCF-7 cells (5×10^4) were seeded in 6-well plates and incubated at 37 °C in 5% CO_2 for 24 h to reach 70% confluence. Various formulations (Blank FA-PAAs, PEI-25k/MMP-9, FA-PAAs/MMP-9 and PAAs/MMP-9) were added and incubated with the cells for 48 h (for protein extraction). In Western blot analysis, transfected cells were washed twice with cold PBS, and then resuspended in 100 μL of lysis buffer (50 mM TriseHCl, pH = 7.4, 150 mM NaCl, 1% Triton X-100, 10% glycerol, 1.5 mM $MgCl_2$, 1 mM EDTA) freshly supplemented with Roche's Protease Inhibitor PMSF Tablets. The cell lysates were incubated on ice for 30 min and vortexed every 5 min. The lysates were then clarified by centrifugation for 10 min at 12 000 r/min. The supernatant was boiled in loading buffer for 10 min. Total protein (20 μL) was separated (at 120 V for 40 min) on 12% PAGE-SDS gels and then transferred (at 300 mA for 40 min) to PVDF membranes (Bio-Rad). After incubation in 5% BSA (Merck, Germany) in phosphate buffered saline with Tween-20 (PBST, pH = 7.2) for 1 h. The membranes were incubated in 5% BSA in PBST with MMP-9 antibodies (1:1000) over night. After incubation in 5% BSA in PBST with goat anti rabbit IgG-HRP antibody (1:5000) for 60 min, bands were visualized using the ECL system (Pierce). Relative protein expression values were determined using Image-J Software.

2.8. Apoptosis assay

MCF-7 cells seeded on the 24-well plates were treated with PAAs, FA-PAAs, PAAs/MMP-9 and FA-PAAs/MMP-9 complexes at 37°C for 48 h. Cells treatment with PBS were used as control. At the end of incubation, all cells were trypsinized, collected and resuspended in 200 μL of binding buffer. Thereafter, 5 μL of V-PE and 10 μL 7-ADD were added and mixed for 15 min in the dark. The stained cells were analyzed using a flow cytometer.

2.9. *In vivo* assay

The Institutional Administration Panel for Laboratory Animal Care (Medical ethics committee of Jinan University) approved the experimental design. The university guidelines for care and use of laboratory animals were strictly followed. All animals were housed and fed in the Experimental Animal Center of Jinan University and were specific pathogen free. Nude mice implanted with

MCF-7 tumors were used for *in vivo* anti-tumor test. The mice were divided into 5 randomized groups, each group comprising 5 mice. Subsequently, the mice were injected through the tail vein with 200 mL PBS (pH = 7.4), blank FA-PAAs, PEI/MMP-9, PAAs/MMP-9 and FA-PAAs/MMP-9. All groups of mice were injected every 2 days. After 3 weeks, the animals were sacrificed.

2.10. Biocompatibility

The cytotoxicity of blank FA-PAAs was studied by CCK-8 assay using MCF-7 cells. The MCF-7 cells were cultured onto a 96-well plate (5×10^3 cells/well) in complete DMEM (with high glucose and 10% fetal bovine serum supplemented) in a humidified atmosphere of 5% CO_2 at 37°C. After 24 h, the growth medium was replaced with 200 μL complete DMEM culture medium that contained the desired amount of FA-PAAs or PEI respectively. Five multiple holes were set for every sample. The cells treated with the same amount of PBS were used as a control group. The cells were incubated for another 48 h, and the cell viability was assayed by adding 20 μL of MTT (Sigma) PBS solution (5 mg/mL). After incubation at 37°C for another 4 h, the formed crystals were dissolved in 150 μL of DMSO. The absorbance that correlated with the number of viable cells in each well was measured by an MRX-Microplate Reader at a test wavelength of 490 nm.

For *in vivo* toxicity study, FA-PAAs (500 mg/kg mouse) was dissolved in PBS and injected into 7 female BALB/c mice (4-week old, 18 ± 2 g) through tail vein, and physiological saline was used as control reagent. After 7 days, all animals were sacrificed, and the liver, heart, brain, spleen and kidney were separated, washed twice with PBS and fixed in 4% formaldehyde for histological examination.

2.11. Blood compatibility

The Institutional Administration Panel for Laboratory Animal Care (Medical ethics committee of Jinan University) approved the experimental design.

2.11.1. Hemolysis

The fresh whole blood was obtained from healthy volunteers by venipuncture using sodium citrate as an anti-coagulant with a blood/anticoagulant ratio of 9:1. The whole blood was immediately centrifuged at 1000 × *g* for 5 min, the resultant plasma and buffy coat layer were removed. The obtained red blood cells (RBCs) were washed with PBS (pH = 7.4) for three times.

Then, the RBCs were suspended in PBS to obtain an RBC suspension at 16% hematocrit (v/v) and mixed with 5 mL PBS containing different FA-PAAs concentrations. Separate positive (100% hemolysis induced by replacing the PBS with 5 mL 0.1% Na_2CO_3 solution) and negative (0% hemolysis, pure PBS without any materials added) controls were set up. Each sample was measured for three times. All samples were incubated for 12 h or 24 h at 37 ℃. After the incubation, the RBC suspensions were centrifuged at 1000 × *g* for 5 min, and the supernatants were measured for the absorbance at 540 nm by using a microplate reader. The percentage hemolysis was calculated by measuring the optical density (OD) as the following formula [29]:

Hemolysis (%) = [(OD of the test sample – OD of negative control) × 100]/OD of positive control.

2.11.2. Activated partial thromboplastin time (APTT) and prothrombin time (PT) assays

The APTT and PT assays were performed on an SF-8000 automatic coagulation analyzer (Beijing Succeeder Company, Beijing, China) with corresponding reagents which were provided by the First Affiliated Hospital of Jinan University (Guangzhou, China). Platelet-poor plasma (PPP) was prepared by centrifuging the citrated whole blood at 1000 × *g* for 15 min and used below. The PPP (180 μL) was mixed with different concentration of M-P-Se (20 μL) and then used for APTT and PT analysis at 37 ℃. Each experiment was repeated for three times. The sample of PPP mixing with PBS was set as control.

Result and discussion

3.1. Synthesis and characterization

FA-modified PAAs was synthesized for targeting gene delivery to tumor cells and the synthetic routes of FA-PAAs is shown in Scheme 1. The bioreducible PAAs was firstly synthesized by Michael addition polymerization of CBA and AEPZ, and then modified by FA through an amidation reaction. The ^{13}C NMR analysis was carried out to confirm the chemical structure of PAAs and FA-PAAs, and the results were shown in Fig. 1. The peaks at 175 ppm were attributed to the carbons from amido bonds. Since peaks in δ 123-133 ppm are typical for carbon of the vinyl groups from CBA [15], the disappearance of those peaks found in both cases indicates the complete end-capping via Michael addition reaction. All of the characteristic peaks of PAAs can be well identified and marked from the spectrum. After conjugation with FA, new peaks appeared at 161 and 165 ppm, which were attributed to the carbons from FA.

UV-Vis spectra analysis was carried out to confirm further the conjugation of FA to PAAs and the FA content in FA-PAAs. Seeing from Fig. 2, FA showed the obvious absorbance peaks at 288 and 365 nm, at which PAAs showed no peaks. This result also indicated that FA-PAAs was synthesized, and the FA content in FA-PAAs was determined as 14.5% by calculating the absorbance value of FA and FA-PAAs.

For GSH-responsibility study, GPC analysis was performed and the chromatograms of FA-PAAs treated with different GSH concentrations were shown in Fig. 3. It was found that FA-PAAs without GSH treatment showed its maximum peak at 8.95 min with the calculated M_n of 31561 (M_n/M_w = 1.69). After incubation with 100 μmol/L GSH for 4 h, the maximum peak of the sample shifted to 10.78 min (M_n = 2217), which indicated that GSH resulted in the breakleadge of disulfide bonds and the obvious degradation of FA-PAAs. When treated with 100 mmol/L GSH for 4 h, the maximum peak of the sample further shifted to 10.98 min (M_n = 693), FA-PAAs degraded further but there was no obvious difference from that treated with 100 μmol/L GSH. This result suggested that FA-PAAs could degrade at the concentration of 100 μmol/L GSH, which was enough for tumor cells therapy because the intracellular concentration of GSH can reach to mmol levels [30].

3.2. FA target

It is reported that FRs are expressed at high levels in breast cancer MCF-7 cells, while expressed at low levels in normal tissues [31]. Due to the strong affinity between FRs and FA, FA-PAAs was expected to facilitate the internalization of the FA-PAAs/DNA complexes into MCF-7 cells.

Fig. 4 showed the cellular uptake ratios of FITC-labeled PAAs and FA-PAAs. It was found that almost 80% PAAs could be uptaken by MCF-7 cells regardless of the concentrations from 0.05 to 0.15 mg/mL, and the FA pretreatment to MCF-7 cells slightly affect the uptaken of PAAs. This indicated that only 0.05 mg/mL PAAs can reach the saturation conditions to MCF-7 cells endocytosis, so the increase of PAAs concentrations would not affect the uptake efficiency. Moreover, PAAs was not FA-targeting, the occupation of FRs did not affect the endocytosis of MCF-7 cells to PAAs. However, the FA pretreatment affect the FA-PAAs uptaken by MCF-7 cells obviously. For normal MCF-7 cells, more than 90% FA-PAAs was uptaken after 1 h incubation.

After MCF-7 cells were pretreated by FA, the uptake ratio of FA-PAAs reduced below 50%. This result indicated the targeting ability of FA-PAAs to high FRs expressed MCF-7 cells. For PAAs, the amount of FRs displayed negligible effect to cellular uptake and the uptake ratios showed no significant difference between FA-pretreated cells and non-FA-pretreated cells. While the cellular uptake ratios for FA-PAAs reduced obviously, because many FRs of MCF-7 cells were occupied by free FA when MCF-7 cells were treated with FA. This occupation affected the interactions between FA-PAAs and MCF-7 cells, and then resulted into the reduction of uptake efficiency.

3.3. *In vitro* transfection

The gene transfection efficiencies of PAAs/MMP-9 (weight ratios of 10, 20 and 30) and FA-PAAs/MMP-9 (weight ratios of 20, 30 and 40) complexes at different N/P ratios with or without serum were evaluated by in vitro gene transfection assay. For a comparative study, PEI-25k/MMP-9 complex was investigated at an N/P ratio of 10, at which PEI-25k could achieve the highest level of transfection efficiency [32]. Fig. 5A showed the *in vitro* transfection results of samples at absence of serum. It was found that both PEI and FA-PAAs showed good MMP-9 delivery ability to MCF-7 cells compared with PAAs. For PEI and FA-PAAs (weight ratio of 30) samples, about 40% MCF-7 cells were transfected and there was no significant difference between them. On the contrary, PAAs showed its best result at the weight ratio of 20 and only 25% MCF-7 cells were transfected. These results indicated the advantage of FA in targeting delivery to MCF-7 cells and facilitated the cellular uptake of FA-PAAs/MMP-9 complexes.

Moreover, the uptaken results shown in Fig. 4 displayed that PAAs and FA-PAAs could be uptaken by MCF-7 cells easily, and there was slight difference in uptaken efficiency between PAAs and FA-PAAs. Nevertheless, the transfection efficiency for PAAs and FA-PAAs decreased obviously. The reason was that for uptaken assays, the uptaken efficiency was recorded once PAAs or FA-PAAs molecules were uptaken by MCF-7 cells. However, for transfection assays, after endocytosis of PAAs/MMP-9 or FA-PAAs/MMP-9, the complexes must escape from lysosome and then dissociated in the cytoplasm. After that, the dissociated MMP-9 then entered into the nucleus to express EGFP [33]. So, there are more obstacles for transfection than only cellular uptake. A series of obstacles resulted in the reduction in transfection efficiency compared with uptake efficiency.

The *in vitro* transfection assay is usually carried out at absence of serum, because the gene carriers easily interact with the proteins in the blood which results in the poor transfection efficiency [34]. Herein, to reflect the advantage of this hyperbranched cationic polymer in gene delivery, the transfection assay was carried out in the presence of serum and the results were shown in Fig. 5B and 5C. It was found that PEI was significantly affected by the serum in gene delivery and the transfection efficiency reduced about 83% compared that at absence of serum. Only 7% MCF-7 cells were transfected by PEI/MMP-9 in the presence of serum. PAAs showed about 48% decrease in transfection efficiency and about 13% MCF-7 cells were transfected with serum at a weight ratio of 20. Although FA-PAAs also showed about 33% decline in transfection efficiency, 27% MCF-7 cells were transfected, which was still much higher than that of PEI and PAAs obviously. Fig. 5C gave the images of MCF-7 cells transfected by different samples, where the tendency was more intuitionistic. The reason of FA-PAAs showing good gene delivery ability may be that FA-PAAs had the targeting ability to MCF-7 cells and conduced to more cellular uptake ratios. Moreover, the modification of FA to PAAs also reduced the zeta potential of FA-PAAs, which may weaken the interactions between FA-PAAs and the proteins in the blood [35].

3.4. Tumor therapy assays

3.4.1. Western blot and apoptosis

To study further the effect of FA-target on the transfection of complexes to MCF-7 cells, western blot analysis was carried out to detect MMP-9 protein expression under the optimized transfection conditions. Fig. 6A showed the image of gel electrophoresis, and the relatively quantitative MMP-9 protein expression result was shown in Fig. 6B. It was found that after sequence-specific MMP-9 gene silencing by complexes, the MMP-9 protein expression level was reduced obviously. Compared with blank FA-PAAs control, all complexes could result in the low expression of MMP-9 protein. Due to the presence of serum in the transfecting process, PEI mediated about 45% reduction of MMP-9 protein, which was not as good as the PAAs and FA-PAAs. Moreover, FA-PAAs showed the best regulation effect with more than 60% expression quantity of MMP-9 protein was inhibited. This result was accordance with that of transfection efficiency.

Many studies have demonstrated that the tumors are closely related to the cellular apoptosis.

When cellular apoptosis is inhibited, the tumors occur and grow. So, most chemotherapy drugs work in cancer therapy through inducing cell apoptosis [36]. MMP-9 protein is one kind of the matrix metalloproteinase, which is highly expressed in tumor cells and plays an important role in tumor growth. So, MMP-9 siRNA was designed to silence the expression of MMP-9 protein and then induce the apoptosis of tumor cells [37,38]. To examine whether FA-PAAs delivered MMP-9 into MCF-7 cells effectively, the percentage of cell apoptosis treated with various formulation of MMP-9 was determined by flow cytometer. Annexin V-PE staining in conjunction with 7-ADD can distinguish early apoptosis from late apoptosis or living cells from necrotic cells. As shown in Fig. 7A and B, blank PAAs and FA-PAAs showed limited apoptosis which indicated their non-cytotoxicity. After incubation with PAAs/MMP-9 for 48 h, MCF-7 cells displayed 24.1% apoptosis. For FA-PAAs/MMP-9 sample, about 33.9% MCF-7 cells apoptosis were observed. This result confirmed that FA-PAAs could target deliver MMP-9 to MCF-7 cells and induce MCF-7 apoptosis, which may be potentially used in cancer therapy.

3.4.2. *In vivo* assay

The *in vivo* anti-tumor effect of FA-PAAs/MMP-9 was tested using MCF-7 tumor-bearing mice as the model animal. PBS and blank samples etc were used as the control groups. The representative tumor images are shown in Fig. 8. As seen, the tumor with PBS-treated increased rapidly, and there was no significant difference in volume with the blank FA-PAAs sample. On the contrary, all the MMP-9-treated groups were effective in tumor regression. FA-PAAs/MMP-9 showed better MCF-7 tumor inhibition than PEI/MMP-9 and PAAs/MMP-9, indicating the superiority of delivering MMP-9 *in vivo*. This result was also in accordance with the western blot and apoptosis results *in vitro*.

3.5. Biocompatibility

3.5.1. Toxicity

As a promising gene carrier for tumor therapy, the cytotoxicity of blank FA-PAAs was evaluated firstly to confirm its safety, and PEI and PBS were set as control groups. MCF-7 cells were chosen to evaluate the cytotoxicity through the CCK-8 assay, and the results were shown in Fig. 9. It was found that FA-PAAs showed low cytotoxicity, and there was no significant difference

in cell viability with PBS control when its concentration was lower than 200 μg/mL. Correspondingly, PEI displayed obvious cytotoxicity to MCF-7 cells and only 30% cells were available when incubated with 60 μg/mL PEI. This result indicated that FA-PAAs showed better safety *in vitro* and is a promising gene carrier in gene therapy to cancers.

In vivo toxicity studies are also carried out through a histological analysis to prove the safety of FA-PAAs used for gene delivery. As shown in Fig. 10, histologically, no visible difference was observed compared to the control (top row). The *in vivo* toxicity of polymers is influenced by the chemical structures, size, exposure duration, biodistribution, location, metabolism as well as the nature of the surface and terminal groups [39]. The toxicity of FA-PAAs also depends on its type, molecular weight and generation. The non-observed toxicity of hyperbranched FA-PAAs could be attributed to its characteristic molecular structure and degradation ability. The hyperbranched structure could reduce the cytotoxicity of polymers compared with linear structure having the similar molecular weights [40]. Moreover, the biodegradability of FA-PAAs can also promote its elimination from cell and organism and thereby enhances their *in vivo* biocompatibility.

3.5.2. Blood safety

As an injectable gene delivery system, the instability of the carriers in the blood was considered as the most serious limitation in the therapeutic, and the nonspecific interactions between carriers and proteins in the blood could severely diminish the bioavailability and target of gene drugs. The blood compatibility of FA-PAAs was assessed by spectrophotometric measurement of hemoglobin release from erythrocytes after FA-PAAs treatment. Fig. 11 showed the percentage hemolysis of the blood in contact with different FA-PAAs concentrations and PEI was set as the control. It was found that FA-PAAs exhibited the good blood compatibility. Even after 24 h incubation with concentrated FA-PAAs up to 1 mg/mL, the sample showed non-hemolytic effect with the extent of hemolysis lower than the permissible level of 5% [34]. However, PEI showed obvious hemolysis, where 1 mg/mL PEI resulted in more than 40% hemolysis.

The effect of gene carriers on blood coagulation is another one of most important functions to blood tissue [41]. Coagulation at the right time and location is necessary to maintain normal metabolism. On the contrary, inappropriate coagulation will cause severe, even lethal, risks to the living system. Therefore, the effect of drug carriers on coagulation is a key factor in the blood safety

evaluation. The blood coagulation cascade contains three types of pathways: intrinsic, extrinsic and common pathway. APTT measures the performance of the intrinsic and common coagulation pathways, and refers to the time required to form a fibrin clot after a partial thromboplastin reagent or $CaCl_2$ is added. PT measures the performance of the extrinsic and common coagulation pathways, and refers to the time to form a fibrin clot after tissue thromboplastin is added [39]. The effects of the FA-PAAs on APTT and PT are shown in Fig. 12. Compared to the PBS control, FA-PAAs did not significant change the APTT and PT of the blood under the concentration of 1 mg/mL. However, PEI with a concentration of 1 mg/mL showed the obvious effect to APTT and PT, which resulted in the no occurrence of blood coagulation. The results indicated that FA-PAAs under experimental concentrations had no obvious activation to coagulation factor XII in the plasma and thrombin, suggesting the blood safety in this work.

4. Conclusion

To deliver MMP-9 siRNA effectively to MCF-7 cells, FA-targeting redox hyperbranched poly(amido amine)s (FA-PAAs) were synthesized. Due to the target ability to MCF-7 cells and intracellular degradation property, FA-PAAs showed excellent transfection efficiency *in vitro*. Particularly, FA-PAAs showed much better gene delivery ability than PEI-25k in the presence of serum, and could mediate an obvious reduction in MMP-9 protein expression and apoptosis of MCF-7 cells. More importantly, FA-PAAs displayed the lower cytotoxicity and better blood compatibility than PEI-25k, suggesting a potential application in gene therapy to tumors.

Acknowledgement

This work was financially supported by National Natural Science Foundation of China (31271019 and 51573071), Natural Science Foundation of Guangdong Province (2014A030313361) as well as the fund from Pearl River S&T Nova Program of Guangzhou (201506010069).

References

1. P. Resnier, T. Montier, V. Mathieu, J. P. Benoit and C. Passirani, *Biomaterials*, 2013, **34**, 6429-6443.

2. Z. Q. Yu, R. M. Schmaltz, T. C. Bozeman, R. Paul, M. J. Rishel, K. S. Tsosie and S. M. Hecht, *J*

Am Chem Soc, 2013, **135**, 2883-2886.

3. A. Balducci, Y. Wen, Y. Zhang, B. M. Helfer, T. K. Hitchens, W. S. Meng, A. K. Wesa and J. M. Janjic, *OncoImmunology*, 2013, **2**, e23034.
4. A. M. Terando, D. M. Agnese and D. R. Holmes, *Ann Surg Oncol*, 2015, **22**, 3225-3229.
5. Y. Wen, H. R. Kolonich, K. M. Kruszewski, N. Giannoukakis, E. S. Gawalt and W. S. Meng, *Mol Pharmaceut*, 2013, **10**, 1035-1044.
6. E. Mohammadifar, A. N. Kharat and M. Adeli, *J Mater Chem B*, 2015, **3**, 3896-3921.
7. A. Koirala, S. M. Conley and M. I. Naash, *Biomaterials*, 2013, **34**, 7158-7167.
8. Y. Wen and W. S. Meng, *J Pharm Innov*, 2014, **9**, 158-173.
9. J. P. Nam, K. Nam, S. Jung, J. W. Nah and S. W. Kim, *J Control Release*, 2015, **209**, 179-185.
10. D. M. Eckmann, R. J. Composto, A. Tsourkas and V. R. Muzykantov, *J Mater Chem B*, 2014, **2**, 8085-8097.
11. P. Kesharwani, V. Gajbhiye and N. K. Jain, *Biomaterials*, 2012, **33**, 7138-7150.
12. X. Du, L. Xiong, S. Dai, F. Kleitz and S. Z. Qiao, *Adv Funct Mater*, 2014, **24**, 7627-7637.
13. R. Cheng, F. Feng, F. H. Meng, C. Deng, J. Feijen and Z. Y. Zhong, *J Control Release*, 2011, **152**, 2-12.
14. X. Du, B. Y. Shi, Y. H. Tang, S. Dai and S. Z. Qiao, *Biomaterials*, 2014, **35**, 5580-5590.
15. Y. Ping, D. C. Wu, J. N. Kumar, W. R. Cheng, C. L. Lay and Y. Liu, *Biomacromolecules*, 2013, **14**, 2083-2094.
16. W. R. Cheng, J. N. Kumar, Y. Zhang and Y. Liu, *Biomater Sci-Uk*, 2015, **3**, 597-607.
17. J. Chen, C. Wu and D. Oupicky, *Biomacromolecules*, 2009, **10**, 2921-2927.
18. K. Jiang, J. Li, J. P. Yin, Q. Ma, B. Yan, X. Zhang, L. Wang, L. F. Wang, T. Liu, Y. L. Zhang, Q. Y. Fan, A. G. Yang, X. C. Qiu and B. A. Ma, *Biomaterials*, 2015, **59**, 77-87.
19. C. L. Shi, X. Guo, Q. Q. Qu, Z. M. Tang, Y. Wang and S. B. Zhou, *Biomaterials*, 2014, **35**, 8711-8722.
20. J. Movellan, P. Urban, E. Moles, J. M. de la Fuente, T. Sierra, J. L. Serrano and X. Fernandez-Busquets, *Biomaterials*, 2014, **35**, 7940-7950.
21. R. D. Dubey, N. Alam, A. Saneja, V. Khare, A. Kumar, S. Vaidh, G. Mahajan, P. R. Sharma, S. K. Singh, D. M. Mondhe and P. N. Gupta, *Int J Pharmaceut*, 2015, **492**, 80-91.
22. E. Gallon, T. Matini, L. Sasso, G. Mantovani, A. A. de Benito, J. Sanchis, P. Caliceti, C.

Alexander, M. J. Vicent and S. Salmaso, *Biomacromolecules*, 2015, **16**, 1924-1937.

23. B. J. Yu, C. Tang and C. H. Yin, *Biomaterials*, 2014, **35**, 6369-6378.
24. F. Zhao, H. Yin and J. Li, *Biomaterials*, 2014, **35**, 1050-1062.
25. J. Y. Wang, B. R. Dou and Y. M. Rao, *Mat Sci Eng C-Mater*, 2014, **34**, 98-109.
26. S. C. Han, W. D. He, J. Li, L. Y. Li, X. L. Sun, B. Y. Zhang and T. T. Pan, *J Polym Sci Pol Chem*, 2009, **47**, 4074-4082.
27. D. Ma, X. Y. Zhou, Y. F. Yang, Y. You, Z. H. Liu, J. T. Lin, T. Liu and W. Xue, *Sci Adv Mater*, 2013, 5, 1307-1315.
28. D. Ma, Q. M. Lin, L. M. Zhang, Y. Y. Liang and W. Xue, *Biomaterials*, 2014, **35**, 4357-4367.
29. Y. Y. Fu, R. S. Hu, C. H. Li, Q. Wang, Z. H. Liu and W. Xue, *J Bioact Compat Pol*, 2014, **29**, 165-179.
30. W. Chen, P. Zhong, F. H. Meng, R. Cheng, C. Deng, J. Feijen and Z. Y. Zhong, *J Control Release*, 2013, **169**, 171-179.
31. X. R. Li, X. C. Yang, Z. Q. Lin, D. Wang, D. Mei, B. He, X. Y. Wang, X. Q. Wang, Q. Zhang and W. Gao, *Eur J Pharm Sci*, 2015, **76**, 95-101.
32. K. Luo, C. X. Li, L. Li, W. C. She, G. Wang and Z. W. Gu, *Biomaterials*, 2012, **33**, 4917-4927.
33. H. M. Aliabadi, B. Landry, C. Sun, T. Tang and H. Uludag, *Biomaterials*, 2012, 33, 2546-2569.
34. D. Zhong, Y. P. Jiao, Y. Zhang, W. Zhang, N. Li, Q. H. Zuo, Q. Wang, W. Xue and Z. H. Liu, *Biomaterials*, 2013, **34**, 294-305.
35. G. Kumar, H. S. Tuli, S. Mittal, J. K. Shandilya, A. Tiwari and S. S. Sandhu, *Tumor Biol*, 2015, **36**, 4005-4016.
36. J. Decock, S. Thirkettle, L. Wagstaff and D. R. Edwards, *J Cell Mol Med*, 2011, **15**, 1254-1265.
37. C. S. Hong, W. Fellows, A. Niranjan, S. Alber, S. Watkins, J. B. Cohen, J. C. Glorioso and P. Grandi, *Gene Ther*, 2010, **17**, 1200-1205.
38. T. Liu, W. Xue, B. Ke, M. Q. Xie and D. Ma, *Biomaterials*, 2014, **35**, 3865-3872.
39. S. Meng, Z. J. Liu, L. Shen, Z. Guo, L. S. L. Chou, W. Zhong, Q. G. Du and J. Ge, *Biomaterials*, 2009, **30**, 2276-2283.
40. A. G. Nurioglu, A. C. C. Esteves and G. de With, *J Mater Chem B*, 2015, 3, 6547-6570.
41. R. K. Kainthan, M. Gnanamani, M. Ganguli, T. Ghosh, D. E. Brooks, S. Maiti and J. N. Kizhakkedathu, *Biomaterials*, 2006, **27**, 5377-5390.

Scheme 1. Synthesis routes to FA-PAAs.

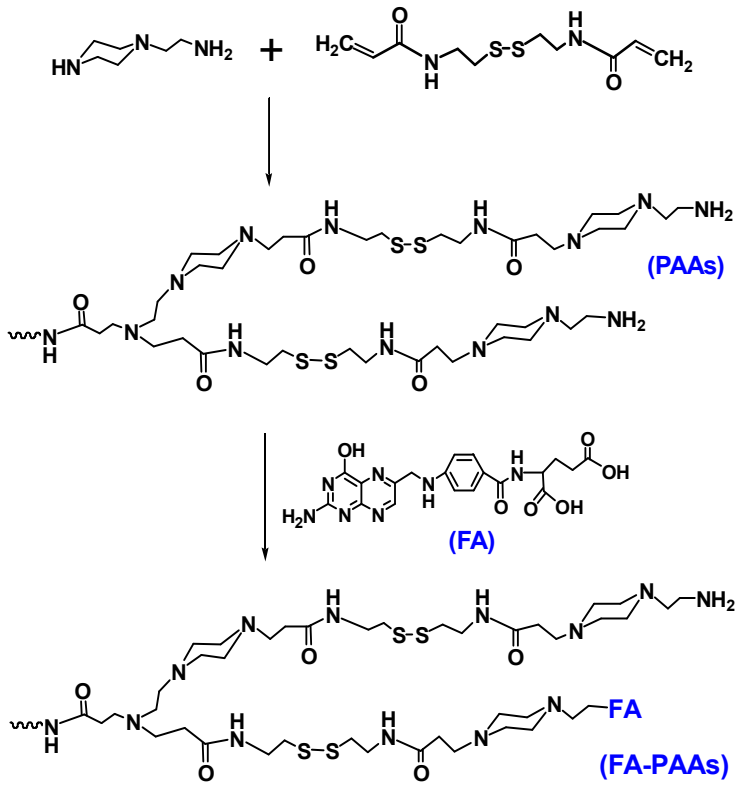

Figure 1. ^{13}C NMR spectrum of FA-PAAs (D_2O, 25°C).

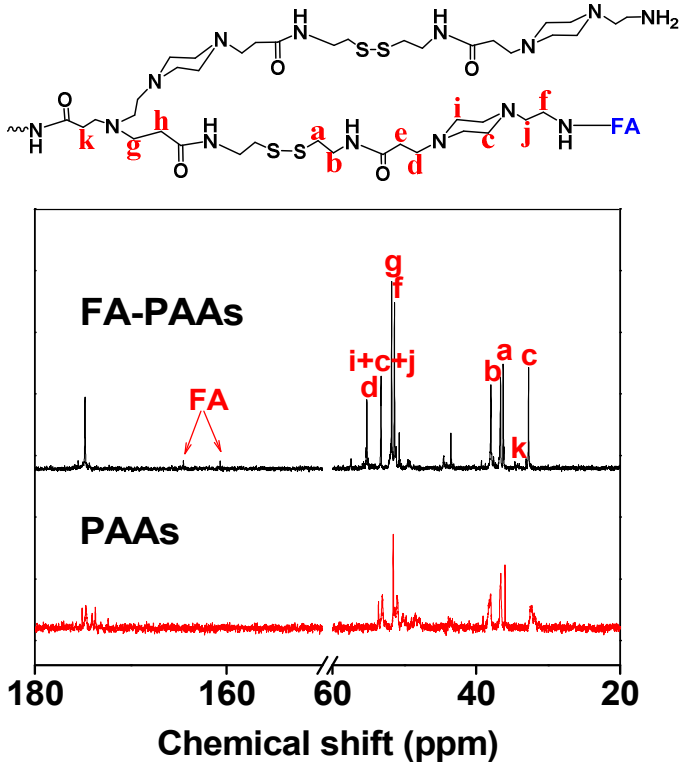

Figure 2. UV-Vis spectra of PAAs, FA and FA-PAAs (25°C).

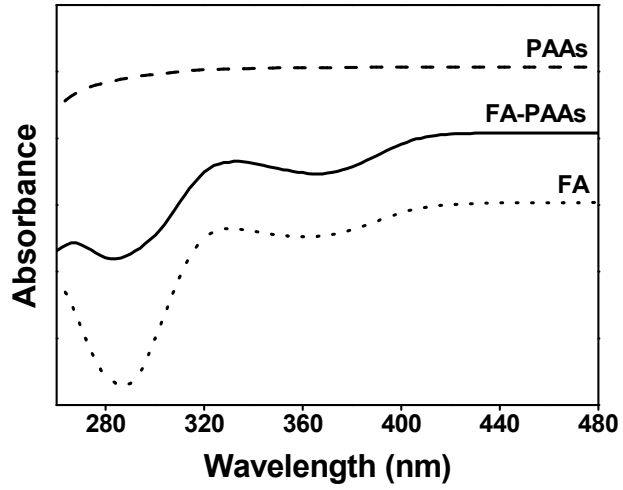

Figure 3. GPC chromatogram of FA-PAAs samples treated with different GSH concentrations (using dextran as the standard sample; 0.8 mol/L $NaNO_3$; 35°C).

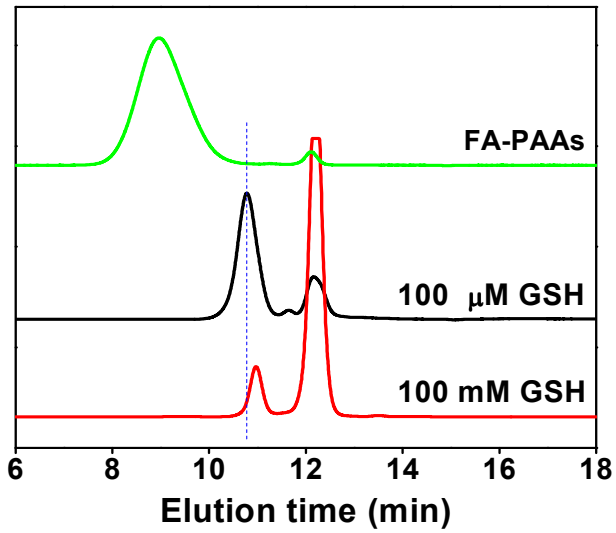

Figure 4. Cellular uptake ratios of PAAs (A) and FA-PAAs (B) after incubated with normal or FA-pretreated MCF-7 cells. (1-3 represent the concentrations of PAAs or FA-PAAs. 1: 0.05 mg/mL; 2: 0.10 mg/mL; 3: 0.15 mg/mL.)

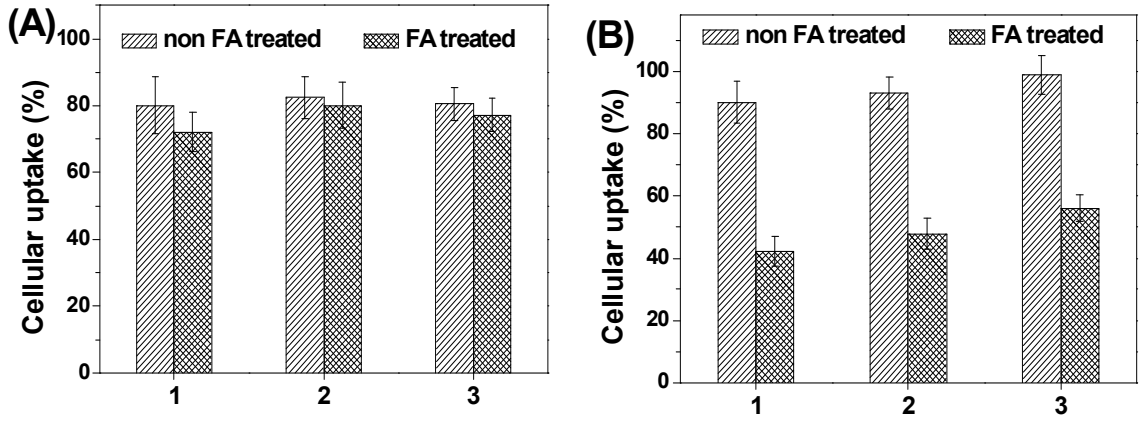

Figure 5. Results of transfected MCF-7 cells at absence (A) or in the presence (B) of serum. (C) Images of transfected MCF-7 cells in the presence of serum.

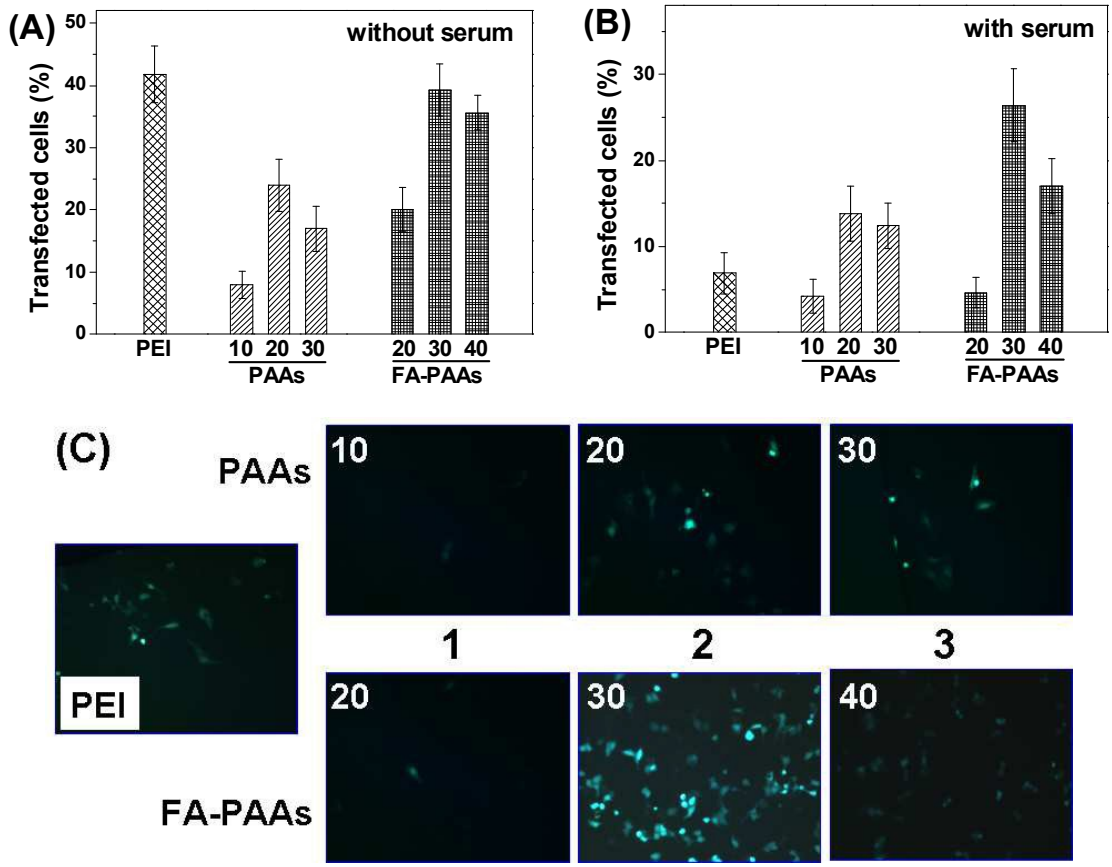

Figure 6. (A) Representative MMP-9 protein expression determined by Western blot analysis. (B) Analysis of light intensities of MMP-9 protein expression as the ratio of MMP-9 to bactin from Western blot results. 1: black FA-PAAs; 2: PEI/MMP-9 (N/P = 10); 3: FA-PAAs/MMP-9 (weight ratio of 30); 4: PAAs/MMP-9 (weight ratio of 20). PBS was set as the control.

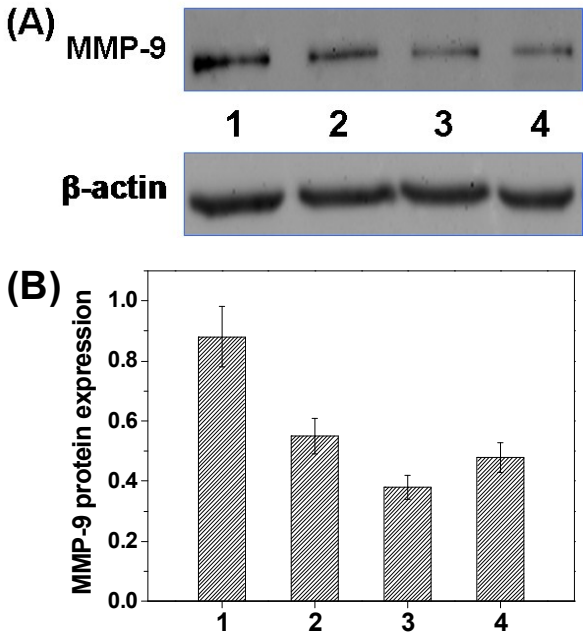

Figure 7. Apoptosis analysis (A and B) by flow cytometry after MCF-7 cells incubated with various samples. 1: PAAs; 2: PAAs/MMP-9 (weight ratio of 20); 3: FA-PAAs; 4: FA-PAAs/MMP-9 (weight ratio of 30). PBS was set as the control.

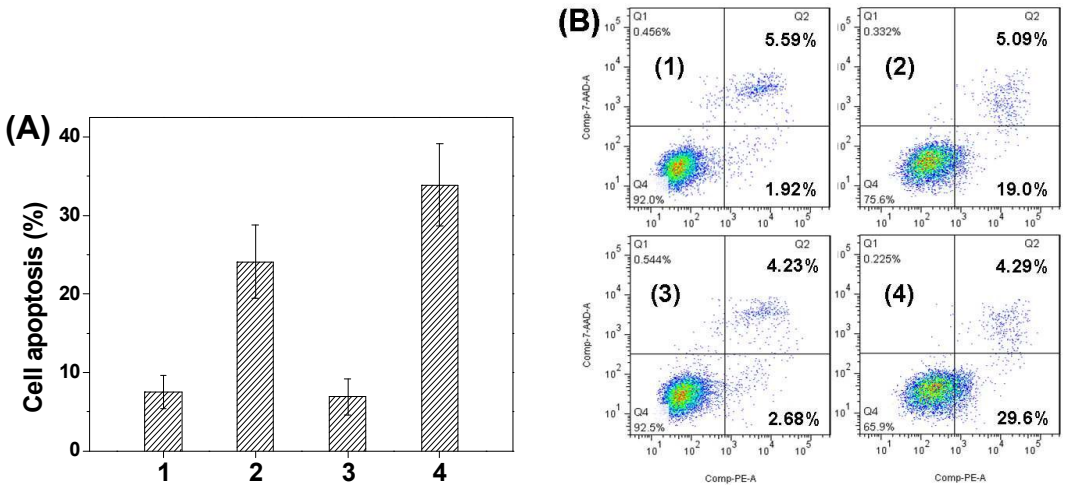

Figure 8. Representative photograph of the MCF-7 tumors at the 21st day after treatment with various formulations.

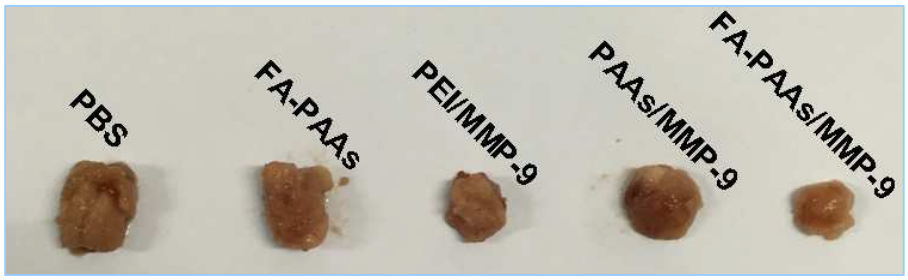

Figure 9. CCK-8 results of FA-PAAs and PEI at different concentrations on MCF-7 cells.

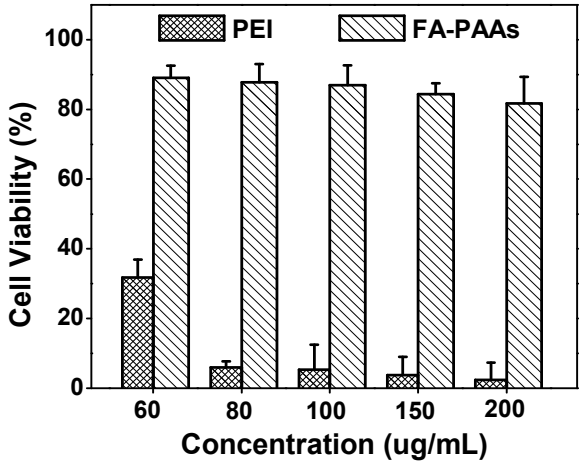

Figure 10. Representative organ histology for control (top row) and FA-PAAs (bottom row) injected mice.

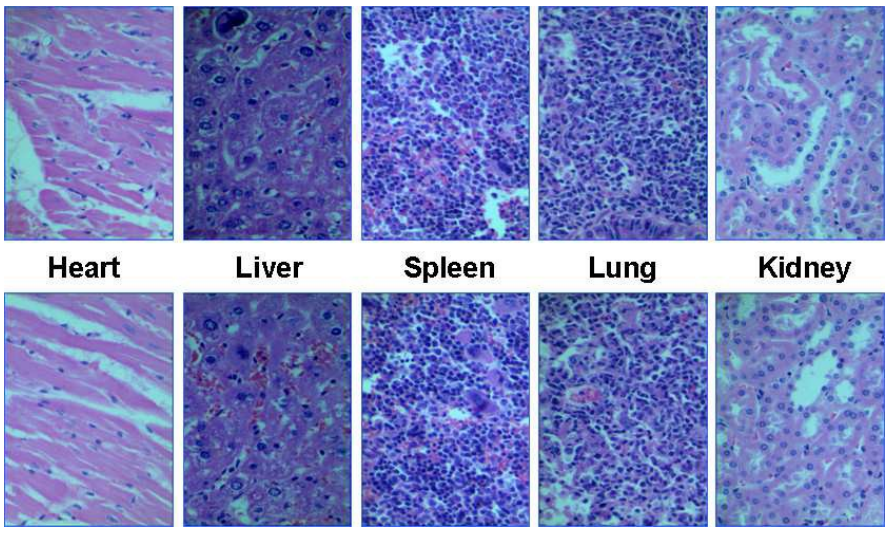

Figure 11. Effect of the concentrations of FA-PAAs and PEI on hemolysis.

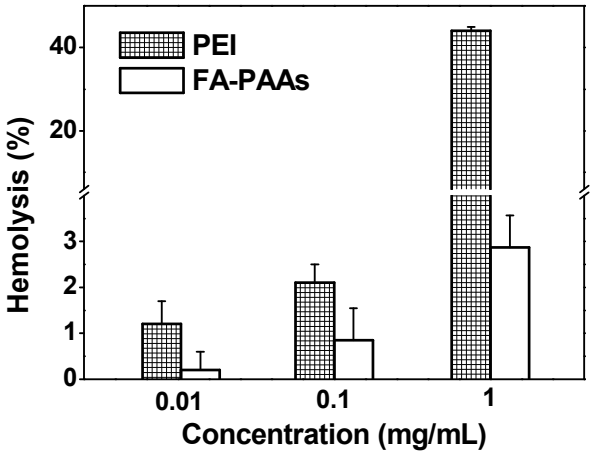

Figure 12. Effect of PEI and FA-PAAs concentrations on APTT (A) and PT (B).

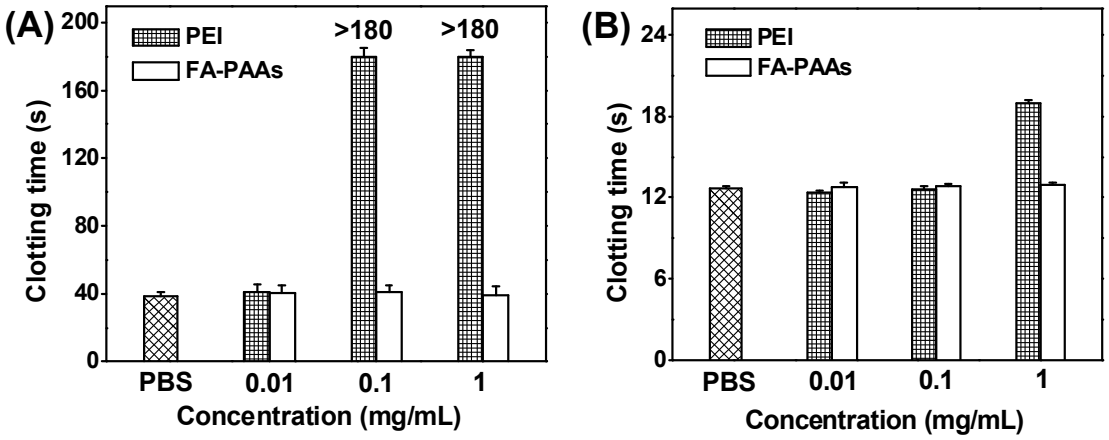

Colour graphic

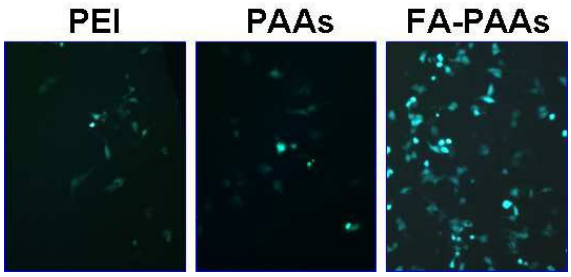

Text

A folated-modified hyperbranched poly(amido amine)s showed much better gene delivery ability than PEI-25k to MCF-7 cells *in vivo*.